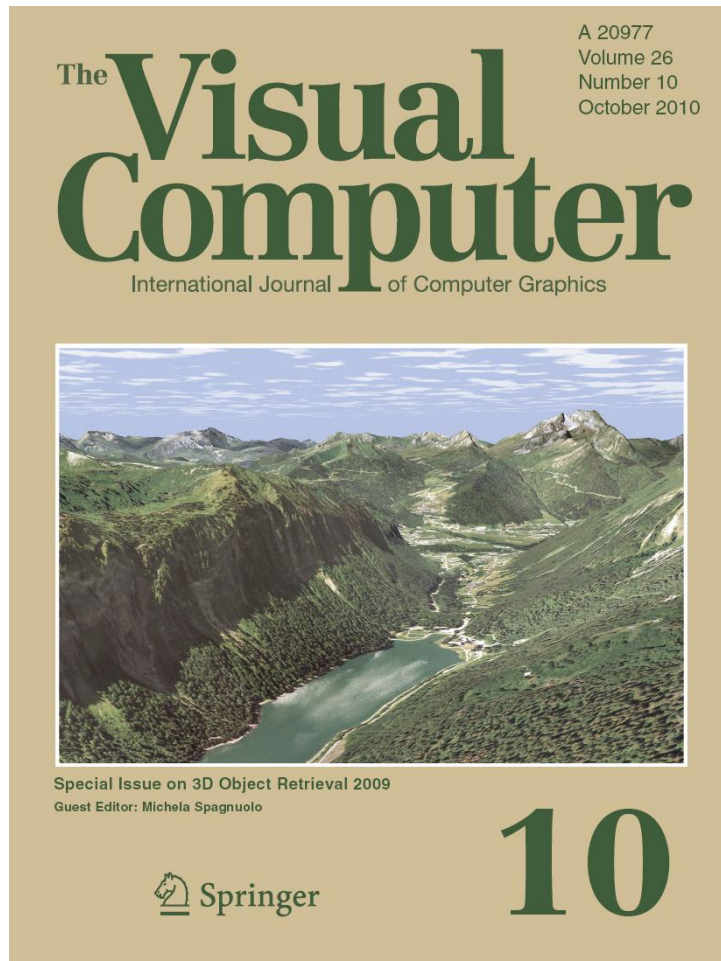


**ISSN 0178-2789, Volume 26, Number 10**



**This article was published in the above mentioned Springer issue.  
The material, including all portions thereof, is protected by copyright;  
all rights are held exclusively by Springer Science + Business Media.  
The material is for personal use only;  
commercial use is not permitted.  
Unauthorized reproduction, transfer and/or use  
may be a violation of criminal as well as civil law.**

# The *bag of words* approach for retrieval and categorization of 3D objects

Roberto Toldo · Umberto Castellani · Andrea Fusiello

Published online: 11 August 2010  
© Springer-Verlag 2010

**Abstract** In this paper, we propose a novel framework for 3D object retrieval and categorization. The object is modeled in terms of its subparts as an histogram of 3D *visual word* occurrences. We introduce an effective method for hierarchical 3D object segmentation driven by the minima rule that combines spectral clustering—for the selection of seed-regions—with region growing based on fast marching. Descriptors attached to the regions allow the definition of the visual words. After coding of each object according to the Bag-of-Words paradigm, retrieval can be performed by matching with a suitable kernel, or categorization by learning a Support Vector Machine. Several examples on the Aim@Shape watertight dataset and on the Tosca dataset demonstrate the versatility of the proposed method in working with either 3D objects with articulated shape changes or partially occluded or compound objects. Results are encouraging as shown by the comparison with other methods for each of the analyzed scenarios.

**Keywords** 3D object retrieval · 3D object categorization · 3D segmentation

## 1 Introduction

In the last years, the proliferation of large databases of 3D models caused a surge of interest in methods for content-

based object retrieval [5, 9, 14, 29]. One of the major challenges in the context of data retrieval is to elaborate a suitable canonical characterization of the entities to be indexed. In the literature, this characterization is referred to as *descriptor* or *signature*. Since the descriptor serves as a key for the search process, it decisively influences the performance of the search engine in terms of computational efficiency and relevance of the results. Descriptors are *global* or *local*. The former consist in a set of features that effectively and concisely describe the entire 3D model [10]. The latter are instead collections of local features of relevant object subparts [27].

In this paper, we exploit the *Bag-of-Words* (BoW) approach in order to combine and merge local information into a global object signature. The BoW framework has been proposed for textual document classification and retrieval. A text is represented as an unordered collection of words, disregarding grammar and even word order. The extension of such approach to visual data requires the building of a *visual vocabulary*, i.e., the set of the visual analog of words. For example, in [6] 2D images are encoded by collecting interest points which represent local salient regions. This approach has been extended in [12] by introducing the concept of *pyramid* kernel matching. Instead of building a fixed vocabulary, the visual words are organized in a hierarchical fashion in order to reduce the influence of the free parameters (e.g., the number of bins of the histogram). Finally, in [16] the BoW paradigm has been introduced for human actions categorization from real movies. In this case, the visual words are the quantized vectors of spatiotemporal local features. The extension of the BoW paradigm to 3D objects is nontrivial and has been proposed only in few recent works [17, 18, 20]. In [20], range images are synthetically generated from the full 3D model and subsequently treated as 2D (intensity) images. In [17, 18], Spin Images are chosen

---

R. Toldo · U. Castellani (✉) · A. Fusiello  
Dipartimento di Informatica, Università di Verona,  
Strada Le Grazie 15, 37134 Verona, Italy  
e-mail: [umberto.castellani@univr.it](mailto:umberto.castellani@univr.it)

R. Toldo  
e-mail: [roberto.toldo@univr.it](mailto:roberto.toldo@univr.it)

A. Fusiello  
e-mail: [andrea.fusiello@univr.it](mailto:andrea.fusiello@univr.it)

as local shape descriptors after sampling the mesh vertices. Usually local techniques are defined by point-based features rather than by segmentation. More recently, a part-based retrieval method [24] have been proposed. The method partitions the object into meaningful segments and finds analogous parts in other objects. Very recently, [8] proposed an approach that uses a collection-aware shape decomposition combined with a shape thesaurus and inverted indexes to cope with the partial matching problem.

In our approach, a 3D visual vocabulary is defined by extracting and grouping the geometric features of the object sub-parts. Thank to this *part-based* representation of the object we achieve pose invariance, i.e., insensitivity to transformations that change the articulations of the 3D object [11]. In particular, our method is able to discriminate objects with similar skeletons, a feature that is shared by very few other works like [3, 19, 28, 30].

Beside being very effective in object retrieval, the BoW representation proved valuable also in the task of 3D object categorization. In particular, we devised a *learning-by-example* approach [7]: Geometric features representing the query-model are fed into a Support Vector Machine (SVM) which, after a learning stage, is able to assign a *category* (or a *class*) to the query-model without an explicit comparison with all the models of the dataset.

In summary, the proposed approach is composed by the following main steps:

Object subparts extraction (Sect. 2). Spectral clustering is used for the selection of seed-regions. Being inspired by the *minima-rule* [13], the adjacency matrix is tailored in order to allow convex regions to belong to the same segment. Furthermore, a multiple-region growing approach is introduced to expand the selected seed-regions, based on a weighted fast marching. The main idea consists on reducing the speed of the front for concave areas which are more likely to belong to the region boundaries. Then the segmentation is recovered by combining the seeds selection and the region-growing steps.

Object sub-parts description (Sect. 3). Local region descriptors are introduced to define a compact representation of each sub-part. Working at the part level, as opposed to the whole object, enables a more flexible class representation and allows scenarios in which the query model is significantly deformed. We focus on region descriptors easy to compute and partially available from the previous step (see [27] for an exhaustive overview of shape descriptors).

3D visual vocabularies construction (Sect. 4). The set of region descriptors are properly clustered in order to obtain a fixed number of 3D visual *words* (i.e., the set of clusters centroids). In fact, the clustering defines a vector quantization of the whole region descriptor space. Note that the vocabulary should be large enough to distinguish relevant changes in object parts, but not so large as to discriminate irrelevant variations such as noise.

Object representation and matching (Sect. 5). Each 3D object is encoded by assigning to each object sub-part the corresponding visual word. The BoW representation is defined by counting the number of object sub-parts assigned to each word. In practice, a histogram of visual words occurrences is built for each 3D object which represent its *global signature* [6]. Matching is accomplished by comparing the signatures.

Object categorization by SVM (Sect. 6). A SVM is trained by adopting a learning by example approach. In particular, a suitable kernel function is defined in order to implicitly implement the subpart matching.

Finally, the proposed approach has been successfully applied on different applicative scenarios, namely (i) 3D object retrieval, (ii) partial shape matching, and (iii) 3D object categorization.

## 2 Objects segmentation

The recent survey by [25] and the comparative study by [1] have thoroughly covered the several different approaches developed in literature.

In the following, we present a novel mesh segmentation technique that provides a consistent segmentation of similar meshes, depends on very few parameters and is very fast. It is inspired by the *minima rule* [13]: “for the purposes of visual recognition, the human visual system divides 3D shapes into parts at negative minima of principal curvature.” Therefore, this suggests to cluster in the same set convex regions and to detect boundary parts as concave ones. A concise way to characterize the shape in terms of principal curvatures is given by the *Shape Index* [22].

$$s = -\frac{2}{\pi} \arctan\left(\frac{k_1 + k_2}{k_1 - k_2}\right) \quad k_1 > k_2, \quad (1)$$

where  $k_1, k_2$  are the principal curvatures of a generic vertex  $x \in V$ . The Shape Index varies in  $[-1, 1]$ : a negative value corresponds to concavities, whereas a positive value represents a convex surface.

The key idea behind our algorithm is the synergy between two main phases: (i) the detection of similar connected convex regions, and (ii) the expansion of these seed-regions using a multiple region growing approach. According to the minima-rule the Shape Index is employed in both phases. An example of extracted seed regions and corresponding segmentation is shown in Fig. 1.

### 2.1 Seed-regions detection by Spectral Clustering

The extraction of the seed-regions is accomplished with Normalized Graph Cuts [26]. This approach has been firstly

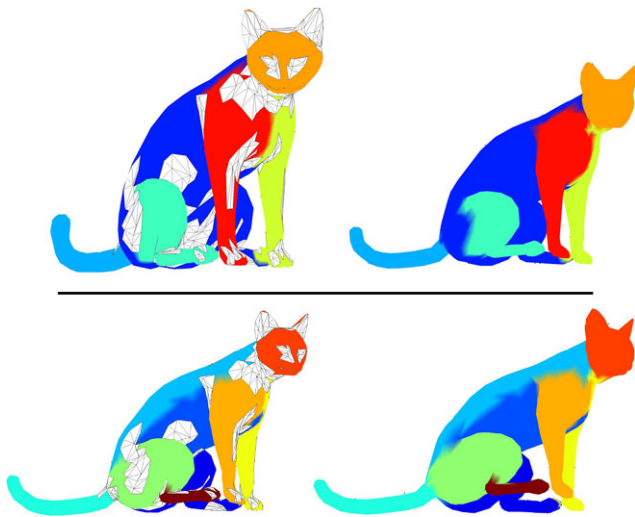


**Fig. 1** An example of segmentation for different number of seeds regions. The starting seeds regions are shown *in left*, while the final segmentations are shown *in right*

applied to image segmentation although it is stated as a general clustering method on weighted graphs. In our case, the weight matrix  $w(x_i, x_j)$  is built using the Shape Index at each vertex:

$$w(x_i, x_j) = e^{-|s(x_i) - s(x_j)|} \tag{2}$$

where the vertices with negative Shape Index—i.e., those corresponding to concave regions—have been previously discarded. In this way, we cluster together vertices representing the same convex shape.

The number of clusters, needed by the Spectral clustering approach, is linked, but not equal, to the number of final segments. Indeed, clusters are not guaranteed to be connected in the mesh. This happens because we do not take into account geodesic distance information at this stage: we cluster only according to the curvature value at each vertex. Hence, we impose connection as a post-processing step: the final seed regions are found as connected components in the mesh graph, with vertices belonging to the same cluster.

### 2.2 Multiple region growing by weighted fast marching

Once the overall seed regions are found, we must establish a criteria to assign the vertices that do not belong to any initial seed region. The key idea is to expand the initial seeds region using a *weighted* geodesic distance. Again, the weight at each vertex is chosen according to the minima-rule. In formulae, given two vertices  $x_0, x_1 \in V$ , we define the *weighted geodesic distance*  $d(x_0, x_1)$  as

$$d(x_0, x_1) = \min_{\gamma} \left\{ \int_0^1 \|\gamma'\| w(\gamma(t)) dt \right\} \tag{3}$$



**Fig. 2** Examples of segmentation of some objects from the Tosca Dataset

where  $w(\cdot)$  is a weight function (if  $w(\cdot) = 1$  this is the classic geodesic distance) and  $\gamma$  is a piecewise regular curve with  $\gamma(0) = x_0$  and  $\gamma(1) = x_1$ . Our weight function is based on the Shape Index  $s$ :

$$w(x) = e^{\alpha s(x)} \tag{4}$$

where  $\alpha$  is an arbitrary constant. A high  $\alpha$  value heavily slows down the front propagation where the concavity are more prominent. In our experiments, we used a fixed  $\alpha = 5$ .

An example segmentation along with starting seed regions is shown in Fig. 1. Several other examples of segmentation on different objects are shown in Fig. 2. The reader might notice how similar parts are segmented in a similar manner (provided that the parameters of the segmentations are equal).

### 3 Segment descriptors

We chose four type of descriptors to represent each extracted region: the Shape Index Histogram (SIH), *Radial Geodesic Distance Histogram* (RGDH), Normal Histogram (NH), and *Geodesic Context* (GC). The first three are defined as the normalized histograms of local measures computed for each point of the region, namely shape index, *radial geodesic distance* and normal. The fourth descriptor depends on the relative positions of the regions, and thus it is a context descriptor.

The *radial geodesic distance* measures the geodesic distance of a surface point to the geodesic centroid of the region. In our case, for computation efficiency, we approxi-

mate the geodesic centroid as the closest point on the mesh to the Euclidean centroid.

The *Geodesic Context* descriptor for a region is built computing the histogram of the geodesic distance between its centroid and the centroids of the other regions. The *GC* descriptor, defined for regions, resembles the shape context descriptor [2], defined for points.

Please note that the number of bins chosen for each histogram of the four descriptors is a critical choice. A small number reduces the capability of the region descriptor in discriminating among different segments. On the other hand, a high number increases the noise conditioning. Hence, we introduce, for each descriptor, histograms with different number of bins in order to obtain a *coarse-to-fine* regions representation.

#### 4 3D visual vocabularies construction

The different sets of region descriptors must be clustered in order to obtain several visual words. Since we start with different segmentations and different types of descriptors, we adopted a multiclustering approach rather than merging descriptors in a bigger set. Before the clusterization, the sets of descriptors are thus split in different subsets as illustrated in Fig. 3. The final clusters are obtained with a *k*-means algorithm. Instead of setting a fixed free parameter *k*, namely the number of cluster, we carry out different clusterizations while varying this value.

Once the different clusters are found, we retain only their centroids, which are our *visual words*. In Fig. 4, an example of descriptors subset clusterization with relative distance

from centroid is shown. Note that object sub-parts from different categories may fall in the same cluster since they share similar shape.

More in detail, at the end of this phase, we obtain the set of visual vocabularies  $V_s^{d,b,c}$  (i.e., *multiple-vocabulary*), where:

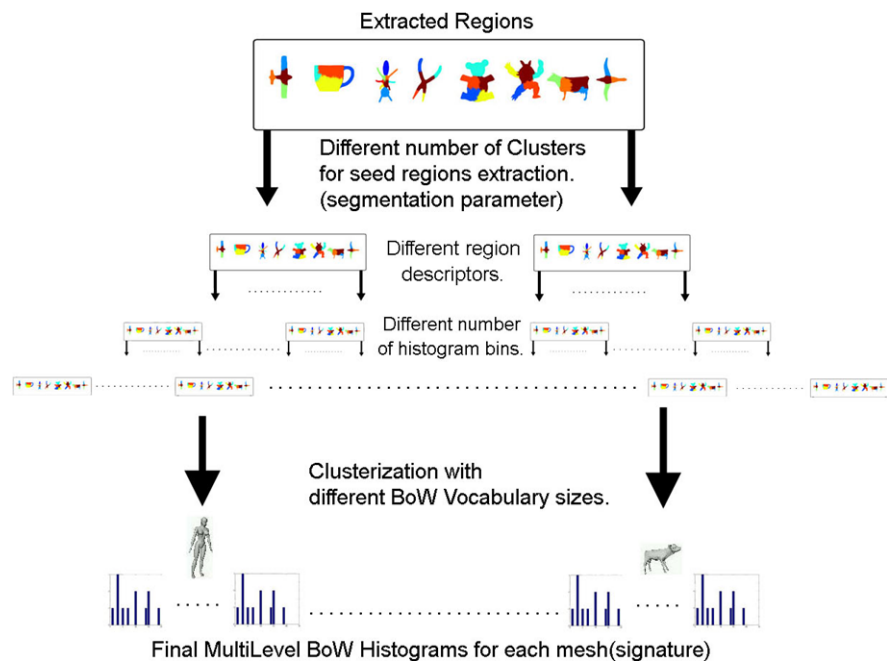
1. *s* identifies the index of the multi-level 3D segmentation (variable segmentation parameter):  
 $s \in \{6, 10, 14\}$
2. *d* identifies the region descriptor types:  
 $d \in \{SIH, RGH, NH, GC\}$
3. *b* identifies the refined level of the region descriptor (number of histogram bins):  
 $b \in \{15, 30, 50\}$
4. *c* identifies the refined level of the vocabulary construction (number of clusters):  
 $c \in \{50, 100, 150\}$

In this fashion, a total of  $3 \times 4 \times 3 \times 3 = 108$  different, nonintersecting visual vocabularies are built. It is worth noting that, in general, the choice of free parameters (i.e., number of bins of a histogram, the number of visual words, and so on), are a critical issue aiming at finding the best trade-off between generalization and overfitting [7]. Here, the values assigned to *s*, *d*, *b*, *c* are heuristically chosen in order to obtain a course-to-fine representation which allow each descriptor to be adaptively represented at its best refined level.

#### 5 3D representation and matching

In order to define a global signature of a new 3D object, we compute the multiple-vocabulary Bag-of-Words representa-

**Fig. 3** The construction of the vocabularies is performed in a multilevel way. At the beginning we have all region extracted for different numbers of seed regions (variable segmentation parameter). For every region, different descriptors are attached. The different region descriptors are divided by the type of descriptor and its number of bins. The final clusterizations are obtained with varying number of clusters. At the end of the process, we obtain different Bag-of-Words histograms for each mesh



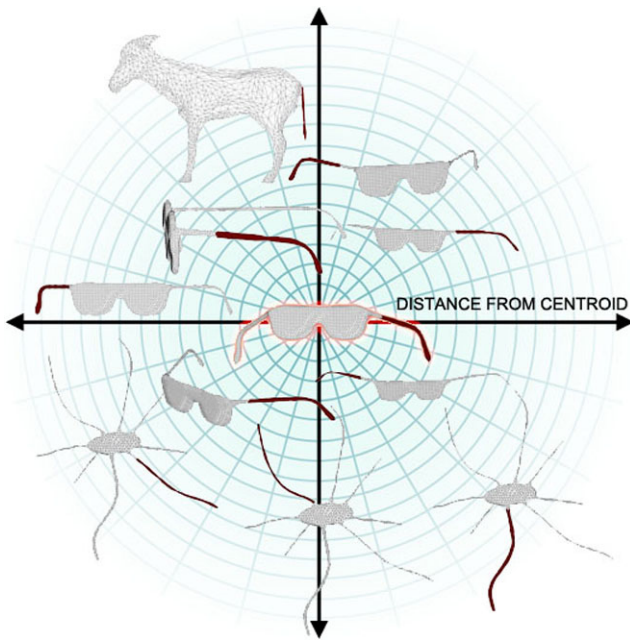


**Fig. 4** Example of a Bag-of-Words cluster for SI descriptors. The centroid is highlighted with red and others region in the same cluster are sorted by distance from centroid. Note that sub-parts of meshes from different categories may fall in the same cluster since they share similar shape

tion. After object segmentation, we compare each region descriptors with the visual words of the corresponding visual vocabulary. More in detail, an object is segmented according to the multi-level segmentation procedure, then each region descriptors is assigned to the most similar words for each (i) level of segmentation, (ii) type of descriptor, (iii) refined level of region descriptor, and (iv) refined level of vocabulary construction. In practice, for an object a Bag-of-Words representation is obtained by counting the number of segments assigned to each word. This procedure is carried out for each of the 108 visual vocabularies, leading to a very sparse signature. Finally, the objects matching is obtained by comparing their respective signature by using standard metric for histograms.

### 6 Object categorization by SVM

One of the most powerful classifier for object categorization is the Support Vector Machine (SVM) (see [4] for a tutorial). The SVM works in a vector space, hence the Bag-of-Words approach fits very well, since it provides a vector representation for objects. In our case, since we work with multiple vocabularies, we define the following positive-semidefinite kernel function:

$$K(A, B) = \sum_{s,d,b,c} k(\phi_s^{d,b,c}(A), \phi_s^{d,b,c}(B)), \tag{5}$$

where  $(A, B)$  is a pair of 3D models, and  $\phi_s^{d,b,c}(\cdot)$  is a function which returns the Bag-of-Words histogram with respect to the visual vocabulary  $V_s^{d,b,c}$ . The function  $k(\cdot, \cdot)$  is in turn a kernel which measures the similarity between histograms  $h^A, h^B$ :

$$k(h^A, h^B) = \sum_{i=1}^c \min(h_i^A, h_i^B), \tag{6}$$

where  $h_i^A$  denotes the count of the  $i$ th bin of the histogram  $h^A$  with  $c$  bins. Such kernel is called *histogram intersection* and it is shown to be a valid kernel [12]. Histograms are assumed to be normalized such that  $\sum_{i=1}^c h_i = 1$ . Note that, as observed in [12], the proposed kernel implicitly encodes the sub-parts matching since corresponding segments are likely to belong to the same histogram bin. Indeed, the histogram intersection function counts the number of sub-parts matching being intermediated by the visual vocabulary.

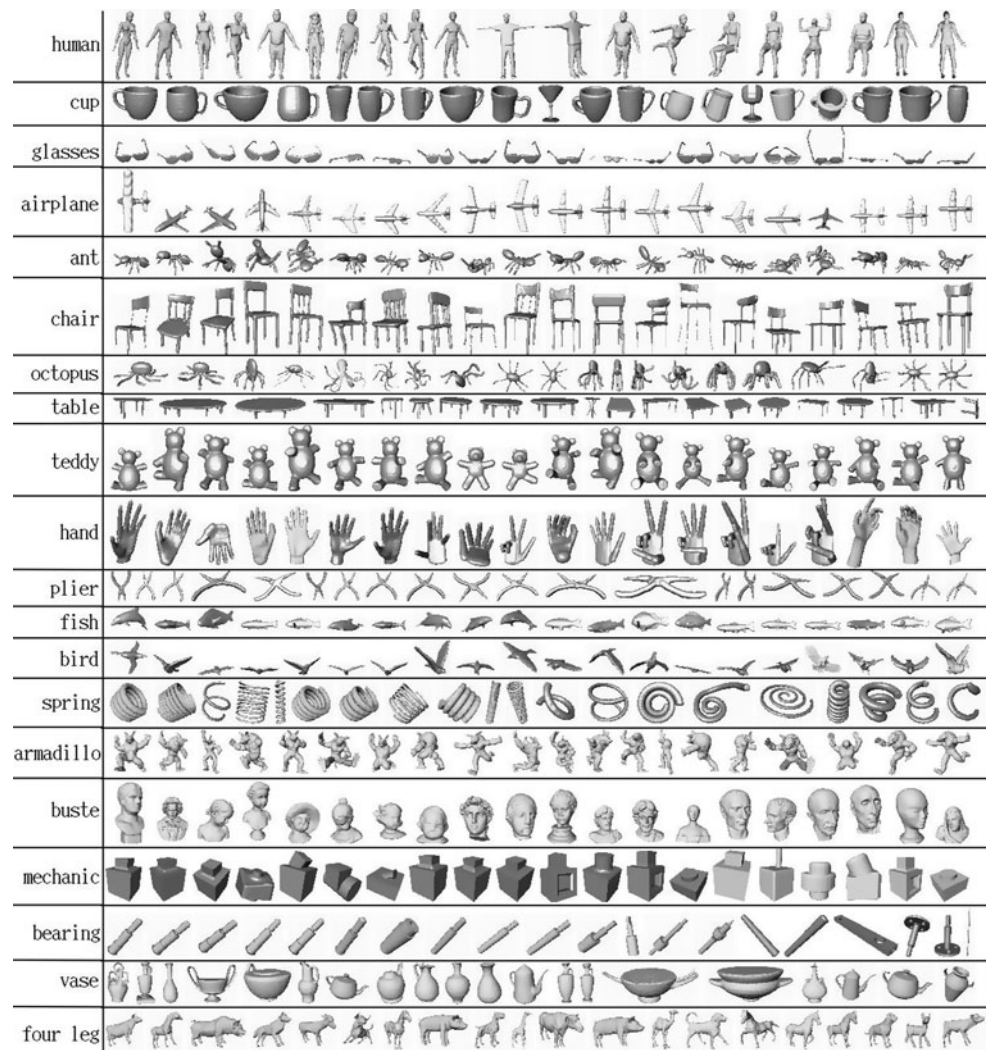
Finally, since the SVM is a binary classifier, in order to obtain an extension to a multi-class framework, a one-against-all approach [7] is followed.

## 7 Results

In order to prove the effectiveness and the generalization capability of the proposed paradigm we tested it with several different retrieval and categorization tasks, also working with compound or partial meshes. The two datasets employed are the Aim@Shape watertight dataset and the Tosca dataset. The first is composed of 400 meshes of 20 different classes (see Fig. 5), with a remarkable inter-class variability. The second is composed of 13 shape classes. In each class, the shape underwent different types of transformations, namely: null (no transformation), isometry, topology (connectivity change obtained by welding some of the shape vertices), isometry + topology, triangulation (different meshing of the same shape) and partiality (missing information, obtained by making holes and cutting parts of the shape). In this case, difficulties arise because the categories are very similar to each other (see Fig. 6 and Fig. 7 for more details).

### 7.1 Aim@Shape Watertight

The Aim@Shape Watertight dataset has been used for various retrieval contests [31]. Firstly, we compared our method with the participant of the Aim@Shape Watertight 2007 contest [31] for object retrieval. We used precision and recall to evaluate our results, that are two fundamental measures often used in evaluating search strategies. Recall is the ratio of the number of relevant records retrieved to the total number of relevant records in the database, while precision

**Fig. 5** Aim@Shape Watertight dataset

is the ratio of the number of relevant records retrieved to the size of the return vector [23]. In Table 2, the precision and recall of our approach along with the results of the other methods are reported, while in Fig. 8 the precision vs. recall plot of our method is shown. The results divided by category are shown in Table 1. The algorithm fails with some meshes, but the overall rate of success is still fairly good.

In the second task, we tested our method with some query test models that are composed of parts of the original dataset. The query test models are 30 and each query model shares common subparts with (possibly) more than one model belonging to the ground-truth dataset. The query set is shown in Fig. 9. Again, we compared our method with the participant of the Aim@Shape Partial Matching 2007 contest [31]. In order to evaluate the performance, a set of highly relevant, marginally relevant and non-relevant models belonging to the dataset has been associated to each query model. The performance indicator used is the Nor-

**Table 1** Precision for each category of the Aim@Shape dataset after 20 retrieved items

Category	Precision after 20	Category	Precision after 20
Human	0.53	Cup	0.46
Glasses	0.90	Airplane	0.73
Ant	0.92	Chair	0.57
Octopus	0.61	Table	0.52
Teddy	0.94	Hand	0.32
Plier	0.99	Fish	0.8
Bird	0.4	Spring	0.96
Armadillo	0.94	Buste	0.57
Mechanic	0.80	Bearing	0.44
Vase	0.8	Four legs	0.32

malized Discounted Cumulated Gain vector (NDCG) [15], which is recursively defined as

$$DCG[i] = \begin{cases} G[i] & \text{if } i = 1, \\ DCG[i - 1] + G[i] \log_2(i) & \text{otherwise,} \end{cases} \quad (7)$$

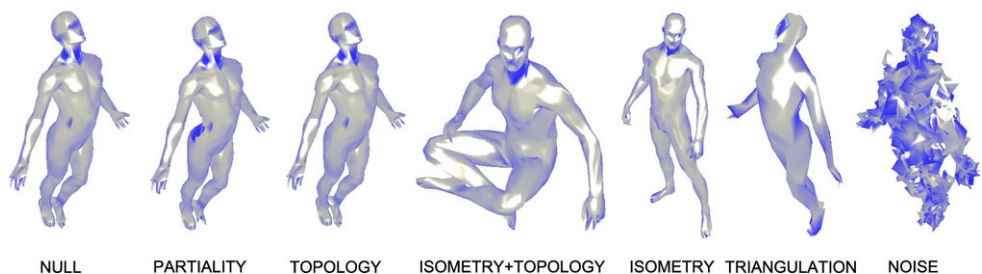
where  $G[i]$  represents the value of the gain vector at the position  $i$ . In our case, for a specific query,  $G[i]$  equals 2 for highly relevant models, 1 for marginally relevant models and 0 for nonrelevant models. The normalized discounted cumulated gain vector NDCG is obtained by dividing DCG by the ideal cumulated gain vector. In Fig. 10 the NDCG of our approach along with the results of the other methods are reported. We can notice how our method performs better than the other methods considered.

Finally, we tested the dataset in a categorization problem. We performed the test using a Leave-One-Out approach. The Overall success rate is high: 87.25%. In Table 3, the different results for each category are reported.



**Fig. 6** Example of different kind of objects in the Tosca dataset. The category are 13, namely: centaur, horse, two males, female, two cats, dog, horse, tiger, elephant, dromedary, and flamingo

**Fig. 7** Example of different type of transformation in the Tosca dataset



## 7.2 Tosca

We tested also the Tosca [21] dataset with a retrieval and a categorization task. In this case, we divided the results for the different type of transformation.

Again, for the retrieval task, we measured the performance using the precision and the recall. In this case, the number of object per category is variable. The query length have thus been made variable according to size of the specific category, so that 1 is the maximum value of precision obtainable. The overall precision is 0.74%.

For the categorization task, the Leave-One-Out validation have been used. The overall success rate is very high: 0.98%.

The precision and the success rate for the categorization task, divided for the different transformation are shown in the Table 4. In Fig. 11, the plot of the precision vs recall for the retrieval task is shown.

## 7.3 Timing and complexity

The entire pipeline is computationally efficient in each stage. We used an entry level laptop at 1.66 Ghz to perform

**Table 2** Precision and recall after 20, 40, 60, and 80 retrieved items for the Aim@Shape dataset

Precision after	20	40	60	80
Ideal	1	0.5	0.333	0.25
Tung et al.	0.714	0.414	0.290	0.225
<b>Our Approach</b>	<b>0.648</b>	<b>0.379</b>	<b>0.270</b>	<b>0.210</b>
Akgul et al.	0.626	0.366	0.262	0.205
Napoleon et al.	0.604	0.366	0.262	0.205
Daras et al.	0.564	0.346	0.252	0.199
Chaouch et al.	0.546	0.329	0.241	0.190
Recall after	20	40	60	80
Ideal	1	1	1	1
Tung et al.	0.714	0.828	0.872	0.902
<b>Our Approach</b>	<b>0.648</b>	<b>0.758</b>	<b>0.808</b>	<b>0.841</b>
Akgul et al.	0.626	0.732	0.786	0.821
Napoleon et al.	0.604	0.732	0.788	0.822
Daras et al.	0.564	0.692	0.756	0.798
Chaouch et al.	0.546	0.658	0.724	0.763



**Fig. 8** Precision vs. Recall for the Aim@Shape dataset

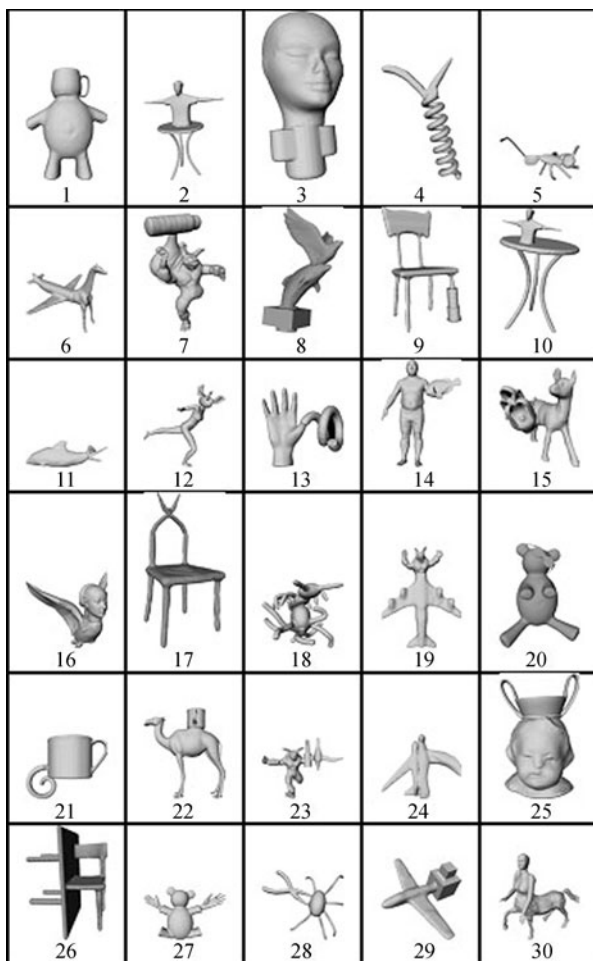
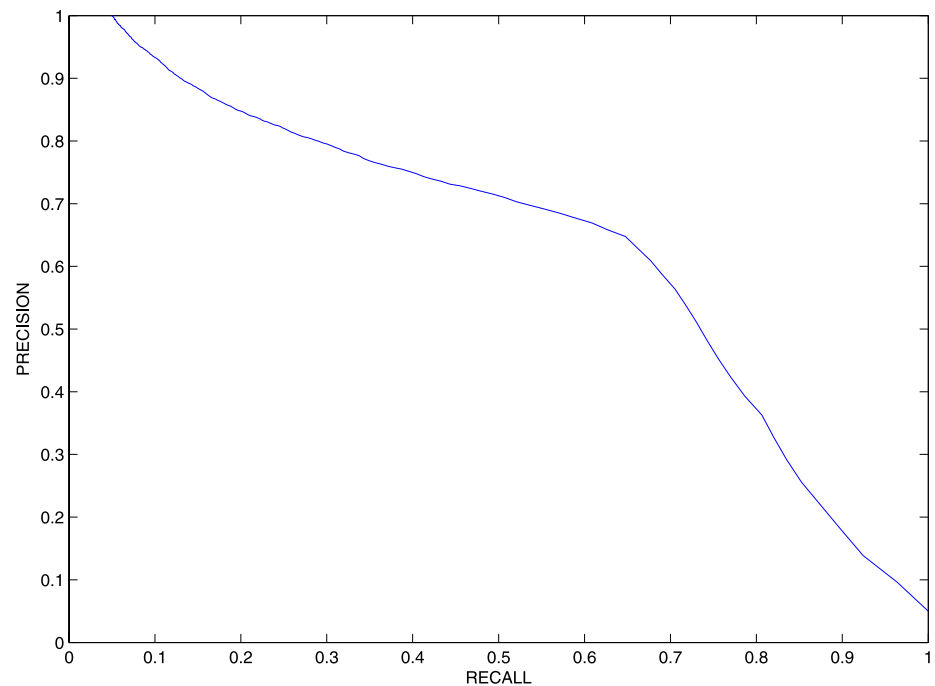


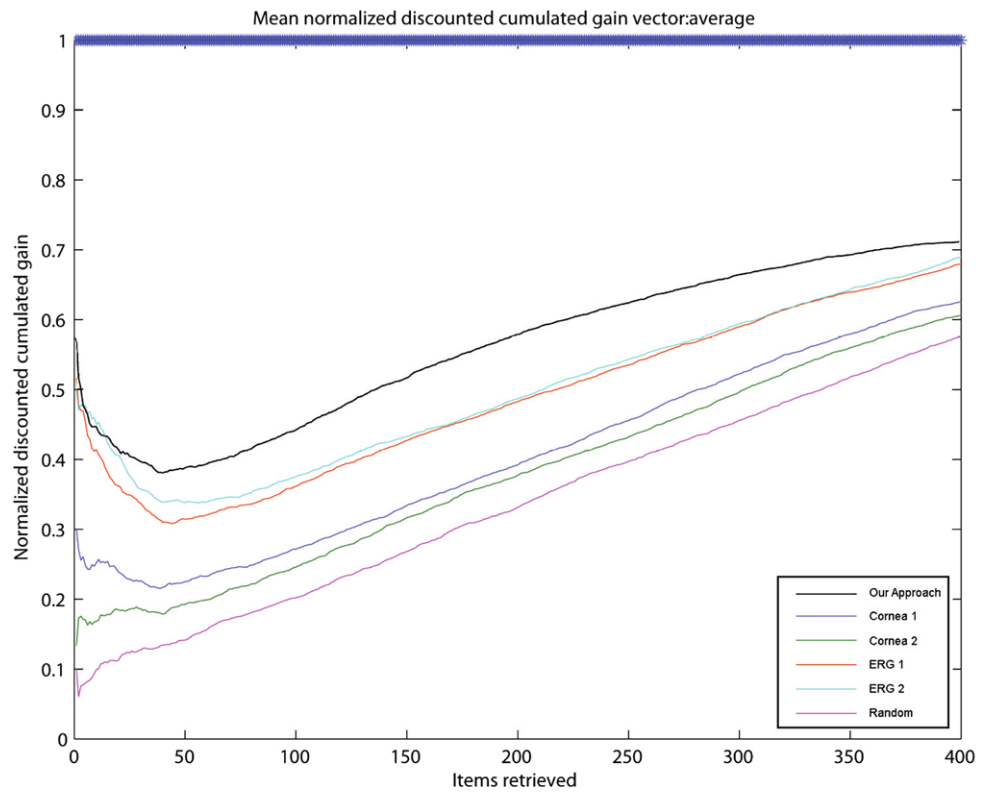
**Fig. 9** Aim@Shape partial matching query objects

**Table 3** Success rate (S.R.) of categorization of the Aim@Shape dataset. The overall rate is **87.25%**

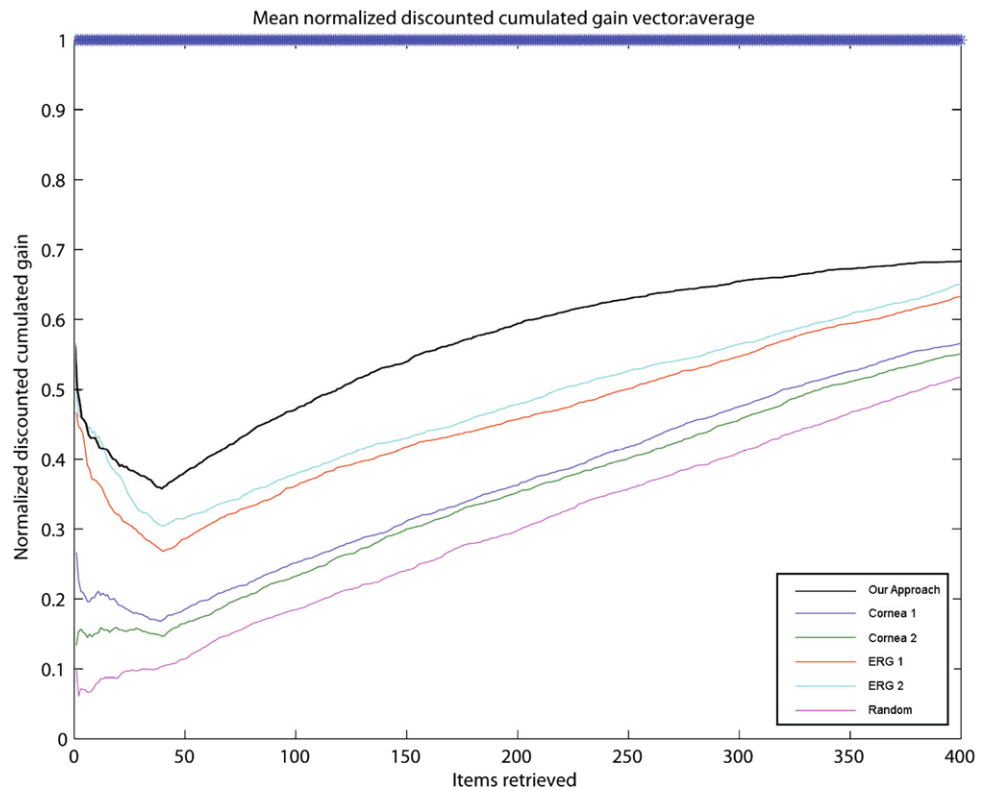
Category	S.R.	Category	S.R.
Human	0.8	Cup	0.85
Glasses	0.95	Airplane	0.9
Ant	1.0	Chair	0.95
Octopus	0.95	Table	0.8
Teddy	1.0	Hand	0.8
Plier	1.0	Fish	0.85
Bird	0.8	Spring	0.95
Armadillo	1.0	Buste	0.95
Mechanic	0.75	Bearing	0.6
Vase	0.75	Four legs	0.8

tests. The code is written in Matlab with some parts in C. The complexity of segmentation depends by the normalized graph cuts algorithm (i.e.,  $n^2$ ) and by fast marching (i.e.,  $n \log n$ ), while the complexity of visual vocabulary construction depends by the  $k$ -means algorithm (i.e.,  $n$  over the number of descriptors). An entire mesh segmentation of 3,500 vertices is computed in less than 5 seconds, of which  $\sim 2.8$  s are necessary to extract all the seed regions, and  $\sim 2.1$  s are needed to compute the entire hierarchical segmentation. Region descriptors are computed efficiently: on the average it takes  $\sim 0.5$  s to extract all the four descriptors of a single region. As for the  $k$ -means clusterization, 10 clusters for 300 points each composed of 200 feature are extracted in less than one second. Finally, the time needed to train a SVM with 400 elements is  $\sim 80$  s, while the time needed to vali-

**Fig. 10** Overall normalized discount cumulated gain considering only highly relevant models (a) and both highly relevant and marginally relevant models (b) for the Aim@Shape partial matching contest



(a)



(b)

**Fig. 11** Precision vs. Recall for the Tosca dataset

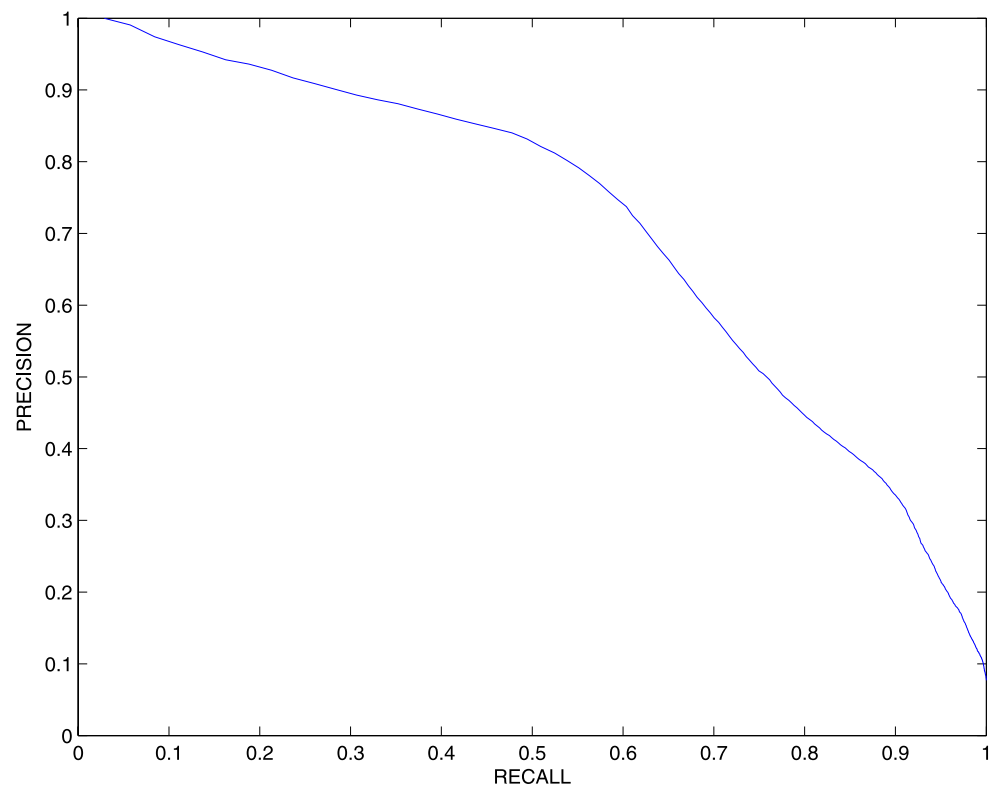


**Table 4** Precision and success rate of the categorization task for the Tosca dataset. The results are divided for type of transformation

Transformation	S.R. precision	S.R. categorization
Isometry	0.77	1.0
Topology	0.44	0.99
Isometry + Topology	0.71	1.0
Noise	0.6	0.8
Null	0.86	1.0
Triangulation	0.58	1.0
Partially	0.68	1.0

date a single element is about  $\sim 2$  s. The overall process, for a dataset composed of 400 elements, takes about 2 hours. The method is super-linear both in the number of vertices of a mesh and in the number of total objects. It is worth noting that, although the time is expected to increase with the number of objects, the proposed method is very local and therefore easily parallelizable.

## 8 Conclusions

In this paper, the Bag-of-Words paradigm has been proposed for the 3D domain. The main steps of the involved processing pipeline have been carefully designed by focusing on both the effectiveness and efficiency.

The Bag-of-Words approach fits naturally with sub-parts encoding by combining segment descriptors into several visual vocabularies. In this fashion, our method is able to satisfy query models of composed objects. Moreover, we have proposed a Learning-by-Example approach by introducing a local kernel which implicitly performs the object subparts matching. In particular, the object categories are inferred without an exhaustive pairwise comparison between all the models.

The experimental results are encouraging. Our framework is versatile in reporting satisfying performances for different applicative scenarios such as object retrieval, partial matching, and shape categorization as shown in the comparison with other methods.

**Acknowledgement** This paper was partially supported by PRIN 2006 project 3-SHIRT.

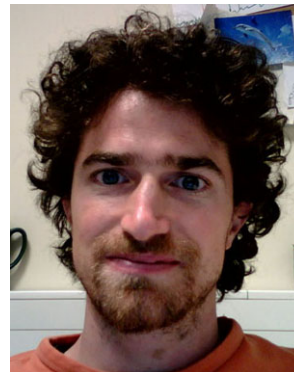
## References

1. Attene, M., Katz, S., Mortara, M., Patane, G., Spagnuolo, M., Tal, A.: Mesh segmentation—a comparative study. In: Proceedings of the IEEE International Conference on Shape Modeling and Applications, p. 7. IEEE Computer Society, Los Alamitos (2006)
2. Belongie, S., Malik, J.: Matching with shape contexts. In: IEEE Workshop on Content-based Access of Image and Video Libraries. Proceedings, pp. 20–26 (2000)
3. Biasotti, S., Marini, S., Spagnuolo, M., Falcidieno, B.: Sub-part correspondence by structural descriptors of 3D shapes. *Comput. Aided Design* **38**(9), 1002–1019 (2006)

4. Burges, C.: A tutorial on support vector machine for pattern recognition. *Data Min. Knowl. Discov.* **2**, 121–167 (1998)
5. Bustos, B., Keim, D., Saupe, D., Schreck, T., Vranić, D.: Feature-based similarity search in 3D object databases. *ACM Comput. Surv. (CSUR)* **37**(4), 387 (2005)
6. Cruska, G., Dance, C.R., Fan, L., Willamowski, J., Bray, C.: Visual categorization with bags of keypoints. In: *ECCV Workshop on Statistical Learning in Computer Vision*, pp. 1–22 (2004)
7. Duda, R., Hart, P., Stork, D.: *Pattern Classification*, 2nd edn. Wiley, New York (2001)
8. Ferreira, A., Marini, S., Attene, M., Fonseca, M., Spagnuolo, M., Jorge, J., Falcidieno, B.: Thesaurus-based 3D object retrieval with part-in-whole matching. *Int. J. Comput. Vis.*, pp. 1573–1405 (2008)
9. Funkhouser, T., Kazhdan, M., Min, P., Shilane, P.: Shape-based retrieval and analysis of 3D models. *Commun. ACM* **48**(6), 58–64 (2005)
10. Funkhouser, T., Min, P., Kazhdan, M., Chen, J., Halderman, A., Dobkin, D.: A search engine for 3D models. *ACM Trans. Graph.* **22**, 83–105 (2003)
11. Gal, R., Shamir, A., Cohen-Or, D.: Pose-oblivious shape signature. *IEEE Trans. Vis. Comput. Graph.* **13**(2), 261–271 (2007)
12. Grauman, K., Darrell, T.: The pyramid match kernel: Efficient learning with sets of features. *J. Mach. Learn. Res.* **8**(2), 725–760 (2007)
13. Hoffman, D.D., Richards, W.A.: Parts of recognition. In: *Cognition*, pp. 65–96 (1987)
14. Iyer, N., Jayanti, S., Lou, K., Kalynaraman, Y., Ramani, K.: Three dimensional shape searching: State-of-the-art review and future trend. *Comput. Aided Design* **5**(37), 509–530 (2005)
15. Järvelin, K., Kekäläinen, J.: Cumulated gain-based evaluation of IR techniques. *ACM Trans. Inf. Syst.* **20**(4), 422–446 (2002)
16. Laptev, I., Marsza, M., Schmid, C., Rozenfeld, B.: Learning realistic human actions from movies. In: *IEEE Conference on Computer Vision and Pattern Recognition* (2008)
17. Li, Y., Zha, H., Qin, H.: Sapetopics: A compact representation and new algorithm for 3d partial shape retrieval. In: *International Conference on Computer Vision and Pattern Recognition* (2006)
18. Lin, X., Godil, A., Wagan, A.: Spatially enhanced bags of words for 3d shape retrieval. In: *ISVC'08: Proceedings of the 4th International Symposium on Advances in Visual Computing*, vol. 5358, pp. 349–358. Springer, Berlin (2008)
19. Cornea, N.D., Demirci, M.F., Silver, D., Shokoufandeh, A., Dickinson, S.J., Kantor, P.B.: 3D object retrieval using many-to-many matching of curve skeletons. In: *IEEE International Conference on Shape Modeling and Applications (SMI05)* (2005)
20. Ohbuchi, R., Osada, K., Furuya, T., Banno, T.: Salient local visual features for shape-based 3d model retrieval. In: *International Conference on Shape Modelling and Applications* (2008)
21. Ovsjanikov, M., Bronstein, A., Bronstein, M., Guibas, L.: Shape Google: a computer vision approach to invariant shape retrieval. In: *Proc. NORDIA* (2009)
22. Petitjean, S.: A survey of methods for recovering quadrics in triangle meshes. *ACM Comput. Surv.* **34**(2) (2002)
23. Salton, G., McGill, M.: *Introduction to Modern Information Retrieval*. McGraw-Hill, New York (1983)
24. Shalom, S., Shapira, L., Shamir, A., Cohen-Or, D.: Part analogies in sets of objects. In: *Eurographics Workshop on 3D Object Retrieval* (2008)
25. Shamir, A.: A survey on mesh segmentation techniques. *Comput. Graph. Forum* (2008)
26. Shi, J., Malik, J.: Normalized cuts and image segmentation. *IEEE Trans. Pattern Anal. Mach. Intel.* **22**(8), 888–905 (2000)
27. Shilane, P., Funkhouser, T.: Selecting distinctive 3D shape descriptors for similarity retrieval. In: *International Conference on Shape Modelling and Applications*. IEEE Computer Society, Los Alamitos (2006)
28. Tam, G.K.L., Lau, W.H.R.: Deformable model retrieval based on topological and geometric signatures. *IEEE Trans. Vis. Comput. Graph.* **13**(3), 470–482 (2007)
29. Tangelder, J.W., Veltkamp, R.C.: A survey of content based 3d shape retrieval methods. In: *International Conference on Shape Modelling and Applications*, pp. 145–156 (2004)
30. Tung, T., Schmitt, F.: Augmented Reeb graphs for content-based retrieval of 3d mesh models. In: *Proc. IEEE Conf. on Shape Modelling and Applications*, pp. 157–166 (2004)
31. Veltkamp, R.C., ter Haar, F.B.: *Shrec 2007 3d retrieval contest*. Technical Report UU-CS-2007-015, Department of Information and Computing Sciences (2007)



**Roberto Toldo** is a Ph.D. student at the Department of Computer Science, University of Verona. He received his *Laurea* degree in Computer Science from the University of Verona in 2008. He has published more than 10 papers on several topics of Computer Vision, including structure and motion, models fitting, 3D registration, and mesh retrieval. His present research is focused on extracting semantic information from sparse points cloud coming from a structure-and-motion process. More details can be found at <http://www.toldo.info/roberto>.



**Umberto Castellani** is Ricercatore (i.e., Research Assistant) of the Department of Computer Science at the University of Verona. He received his Dottorato di Ricerca (Ph.D.) in Computer Science from the University of Verona in 2003 working on 3D data modelling and reconstruction. During his Ph.D., he had been a Visiting Research Fellow at the Machine Vision Unit of the Edinburgh University, in 2001. In 2007, he was an Invited Professor at the LASMEA Laboratory in Clermont-Ferrand, France. In 2008,

he was a Visiting Researcher at the PRIP Laboratory at Michigan State University (USA). His research is focused on 3D data processing, statistical learning, and medical image analysis. He has coauthored several papers which were published in leading conference proceedings and journals. He is a member of Eurographics and IEEE.



**Andrea Fusiello** received his *Laurea* degree in Computer Science from the Università di Udine, Italy in 1994 and his Ph.D. in Information Engineering from the Università di Trieste, Italy in 1999. He worked with the Computer Vision Group at IRST (Trento, Italy) in 1993–1994, and with the Machine Vision Laboratory at the Università di Udine from 1996 to 1998. He was a Visiting Research Fellow in the Department of Computing and Electrical Engineering of Heriot–Watt University (UK) in 1999. Since the year

2000, he has been with the Dipartimento di Informatica, Università di Verona, Italy. Currently, he holds the position of Associate Professor and teaches Computer Vision and Computer Graphics. He has published more than 60 papers on several topics of Computer Vision, including image rectification, tracking, autocalibration, stereopsis, 2-D, and 3-D image registration. His present research is focused on structure-and-motion and 3-D model acquisition from images. Further information can be found at <http://profs.sci.univr.it/~fusiello>.